



February 12, 2013

Mr. Brian Clarke  
Department of Geosciences  
408 Deike Building  
University Park, PA 16802

Subject: Results of Well Logging  
Shale Hills  
Petersburg, PA 16669  
ARM Project: 13129

Dear Mr. Clarke,

ARM Geophysics (ARM) is pleased to present this letter report that summarizes the results of borehole geophysical logging performed at the above referenced site on February 8, 2013. The following standard well logs and borehole images were acquired.

#### LOGGING METHODS

The logs that were run for this investigation include:

Natural Gamma	Single Point Resistance
Fluid Temperature	Spontaneous Potential (SP)
Specific Conductance	Optical Televierer (OTV)
3-Arm Caliper	Acoustic Televierer (ATV)
Short & Long Normal Resistivity	Density
Neutron	Sonic

A summary of these logging methods is provided in Attachment A. The standard logs and ATV were acquired using a MGX II and Matrix acquisition systems manufactured by Mount Sopris Instrument Company. The optical televierer data were acquired using a Robertson Geologging High-Resolution Optical Televierer (HiOPTV) probe and Micrologger 2 acquisition system.

#### BASIC LOG DESCRIPTIONS

The geophysical well logs acquired during this investigation are presented in Attachment B. All log depths are referenced to ground surface as indicated in the header of each log. The majority of the acquired data are presented as standard curves that represent the change in measured parameter with depth. The format of the televierer logs may be less familiar and are therefore further discussed in the following paragraphs.

The televierer logs contain borehole images and structural information obtained from the OTV and ATV tool. The *Optical View* track is an “unwrapped” photographic image of the borehole wall (Figure 1). In this case, the cylindrical borehole

surface is unzipped along the north azimuth and unrolled to a flat strip. The compass orientation (with respect to true north) is presented at the top of the log. The unwrapped format is distorted like any projection of a curved surface on a flat one. Horizontal and vertical planes will be undistorted. However, dipping planes will be represented as a sine wave: the greater the dip, the greater the wave amplitude.

The *Acoustic Amplitude* and *Travel Time* tracks are presented in a similar fashion. The *Acoustic Amplitude* log is a 360° image of the strength or amplitude of the reflected pulse. Lighter colors indicate harder or more competent rock, while darker colors represent fractures and less competent rock. The *Travel Time* data is similar to sonar and represent the travel time of the acoustic pulse as it travels from the tool to the borehole wall and back. This information serves a high resolution and 360° caliper that can indicate the relative lateral depth or openness of fractures.

The Plane Projection track presents the fracture signatures that are digitized from the unwrapped *Optical View* and *Acoustic Amplitude* tracks. The *Dip & Dip Direction* log is a presentation in which the vertical axis is depth and the horizontal is dip angle from 0° to 90°. As shown in Figure 2, the dip direction is indicated by the orientation of the tadpole tail, measured in a clockwise direction from north.

## INTERPRETATION OF STRUCTURAL DIAGRAMS

The structural data are presented on polar and rose diagrams for statistical analysis and pattern visualization. Polar diagrams are used in this report to plot the dip and dip direction of planar features. Zero degree dip is represented at the center of the diagram and 90° at the circumference. The dip direction is indicated by the compass azimuth, measured clockwise from north (0°), as shown in Figure 3. This format is sometimes referred to as a *dip vector plot* but it is essentially the same as a stereonet with an upper hemisphere projection.

The rose diagram graphically illustrates the strike distribution of a set of planes. Radiating rays are drawn with lengths proportional to number of strike measurements within each 10° sector. It is important to recognize that in this report, the polar diagram represents dip and dip direction, whereas the rose diagram represents strike. Using the right-hand-rule convention, strike equals the dip direction minus 90°.

## RESULTS AND DISCUSSION

Optical and acoustic televiewer images were used to measure the depth and orientations of fractures and bedding planes. The measured fracture and bedding plane projections and orientations are shown on the televiewer logs and in the depth track of the HydroLogs. A tabulated listing of the plane orientations is presented in Attachment C. Stereographic analysis was performed on the planar orientation data. The results are presented in the polar and rose diagrams shown in Figures 4 through 6. Predominant groups or “sets” are indicated by the clustering of data points in the polar diagrams. Table 1 lists orientations for all plane sets.

Figure 4 presents a polar diagram showing the dip and dip direction of all planes measured during this investigation. The planes are classified by symbols corresponding to bedding, broken zones, faults, and both open and filled fracture planes. Broken zones are portions of the borehole wall that are fractured in such a way that a sinusoidal plane does not fit. The fault is defined as a fault due to the offset seen in the fracture above and below.

Figure 5 presents a polar diagram with statistical contouring of open fracture plane orientations. Two main sets of fractures were identified. The mean fracture dip/directions of 50/314 and 66/145 are shown to the right of the diagram. Figure 6 presents a rose diagram showing the strike distribution of fracture planes. The results indicate a predominant NE strike direction.

Bedding planes identified were flat, with zero dip. The small number identified combined with the lack of dip/dip direction did not provide sufficient information to create a meaningful structure diagram.

Table 1: Mean orientations of planes.

Type	Dip / Direction	Strike/Dip
Fracture Planes 1	50/314	N44E/50NW
Fracture Planes 2	66/145	N55E/66SE

#### INTERPRETATION OF WATER PRODUCING OR RECEIVING ZONES

Water level was consistently around 58 feet below ground level for all logging runs. Based on the characteristics listed below, Table 2 shows potential transmissive zones.

Water producing or receiving zones are typically identified in the acquired logs by a combination of the following parameters:

- A. Open fractures observed in televiewer data.
- B. Deflections in caliper curve (suggests fractures).
- C. Deflections or change in slope in fluid temperature or fluid resistivity curve.
- D. Decrease in formation resistivity.

Table 2: Potential Transmissive Zones

Depth	Parameters Observed
58-60	A, C, D
69-72	A, C, D
74-75	A, C, D
80-86	A, C, D

#### SONIC DATA

Water level of the DC9 limited sonic data collection to the bottom 40' of borehole. Waveforms for near and far receiver are shown on the log, as well as waveform velocities. The zones around 70' and 82' coincide with highly fractured zones as seen in the televiewer logs.

## DENSITY AND NEUTRON DATA

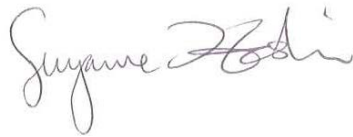
The Density Neutron log also has gamma ray, caliper and image data plotted to assist in getting a larger view of the data. Please note the significant shift in the density and neutron curves at the gas-liquid contact around 60 feet, where water level is.

## CLOSING

The data collection and interpretation methodologies used in this investigation are consistent with standard practices applied to similar geophysical investigations. The correlation of geophysical responses with probable subsurface features is based on the past results of similar surveys although it is possible that some variation could exist at this site.

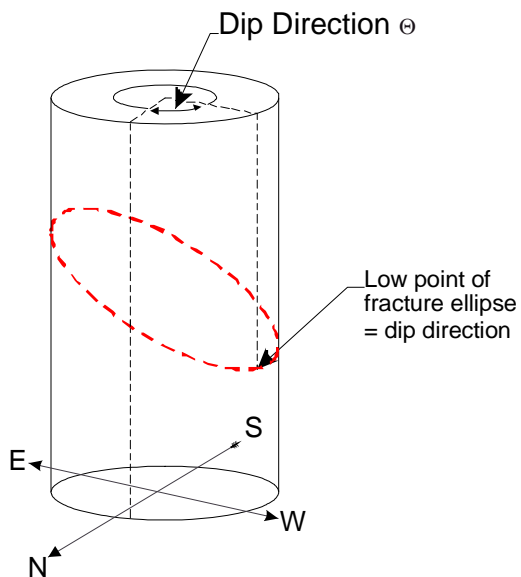
Please contact us if you have any questions regarding this survey. We appreciate your business and look forward to working with you again.

Kind regards,  
ARM Geophysics

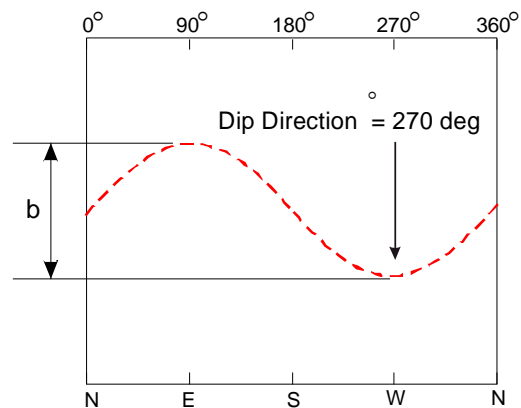
A handwritten signature in cursive script, appearing to read 'Suzanne Heskin'.

Suzanne Heskin  
Senior Geophysicist

## FIGURES



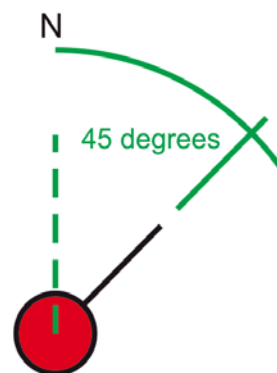
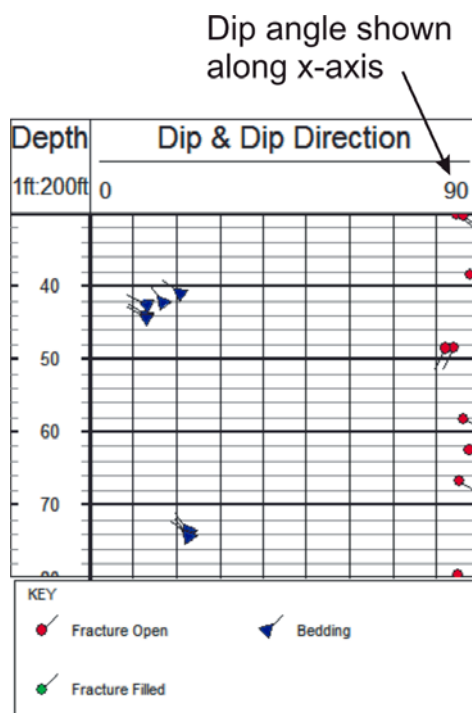
## Unwrapped View



$$\text{Dip} = \arctan \frac{b}{\text{diameter}}$$

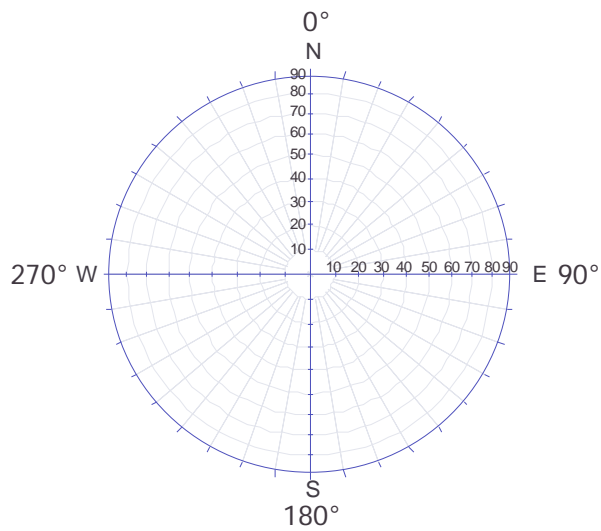
$$\text{Strike} = \Theta \pm 90$$

Figure 1: Diagram illustrating unwrapped view of fracture signature.

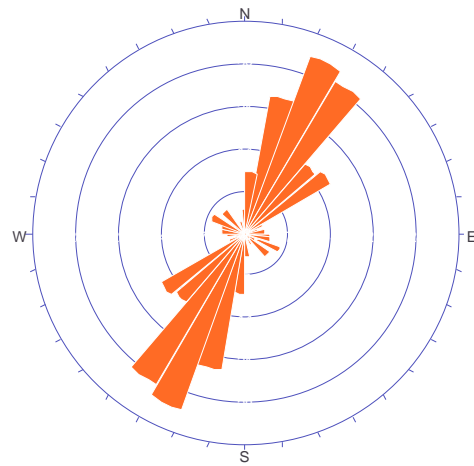


Dip direction indicated by tail orientation

Figure 2: Dip & dip direction determination from the tadpole plot.



Polar Diagram



Rose Diagram

Figure 3: Example polar and rose diagrams. Polar diagram is used in this report for plotting dip and dip direction. Rose diagrams are used for plotting the frequency or number of strike measurements per sector.

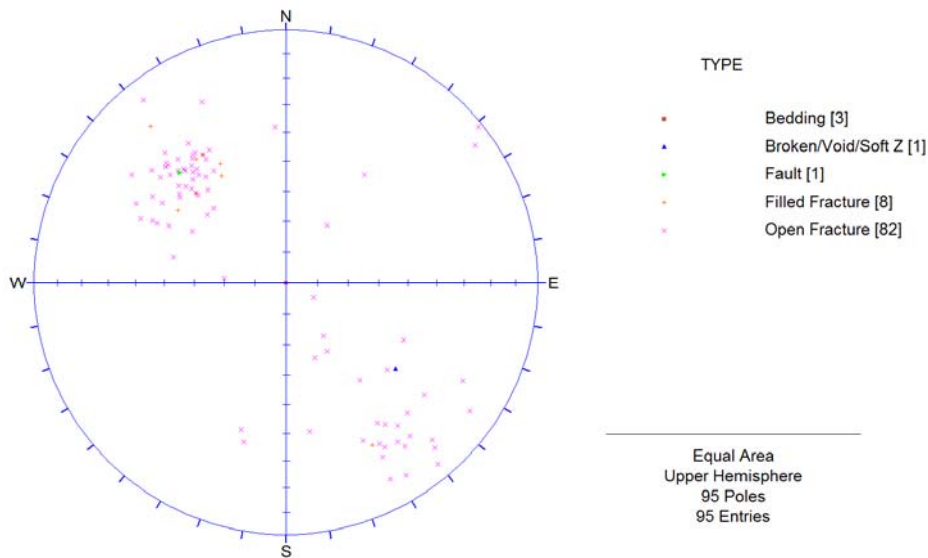


Figure 4: Polar diagram plotting dip and dip direction of all planes categorized by plane type.

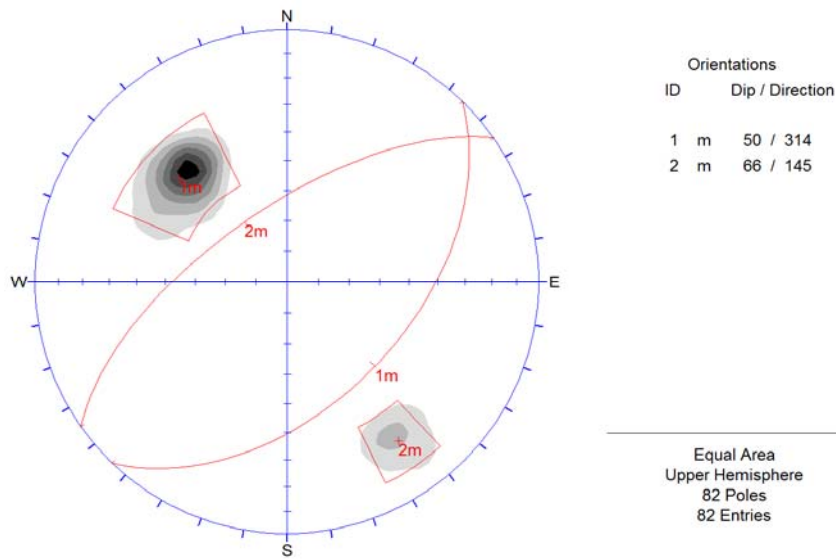


Figure 5: Polar diagram with statistical contouring of fracture plane sets. Calculated mean dip angle and direction is shown at the right of the diagram.

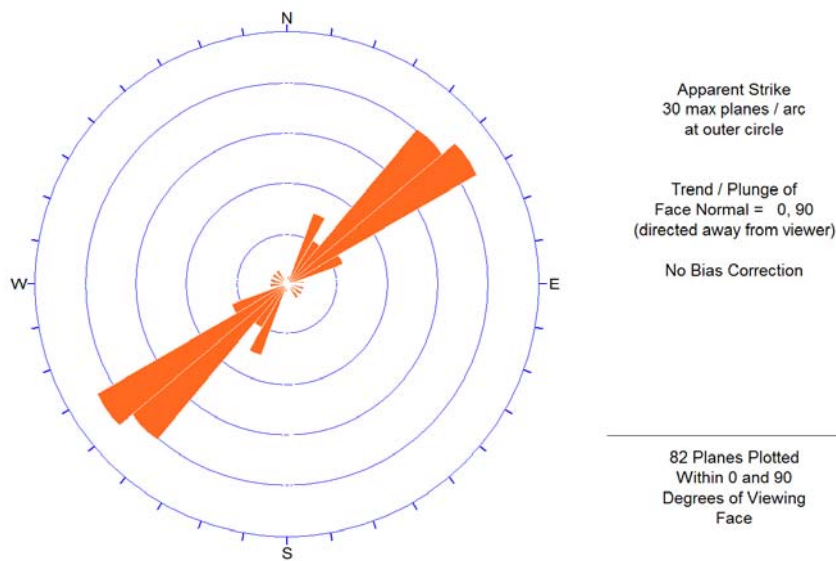


Figure 6: Rose diagram illustrating strike distribution of fracture planes.



ATTACHMENT A  
LOGGING METHODS

## APPENDIX A: OVERVIEW OF LOGGING METHODS

### CALIPER LOGS

The caliper log measures variations in borehole size as a function of depth in a well. Some example responses of in a caliper log is shown in Figure A- 1 (Rider, 2002<sup>1</sup> ) The log data enables (a) the detection of competent or fractured geologic units, (b) the location of washouts or tight zones, (c) the optimal placement of well screen, sand, and bentonite, and (d) the establishment of appropriate borehole correction factors to be applied to other well log curves. Further, when run in combination with other logs, the caliper log may be an indicator of lithologic makeup and degree of consolidation. The typical caliper response in a fractured, weathered, or karstic unit is a relatively abrupt increase in borehole size.

### SPONTANEOUS POTENTIAL (SP) LOGS

The SP log measures the natural voltages that are created within the borehole due to the presence of borehole fluids, formation fluids, and formation matrix materials. It is recorded by measuring the difference in electrical potential in millivolts between an electrode in the borehole and a grounded electrode at the surface. The SP log is commonly used to 1) detect permeable beds, 2) detect boundaries of permeable beds, 3) determine formation water resistivity, and 4) determine the volume of shale in permeable beds. The constant SP readings observed in thicker shale units define the shale base line, a reference line from which further formation matrix and formation fluid property calculations may be completed. Although this log is consistently used in oil and gas applications, its effectiveness in water wells is limited since the method requires a contrast in salinity between borehole and formation fluids (Figure A- 2). This condition is often not met in ground water wells.

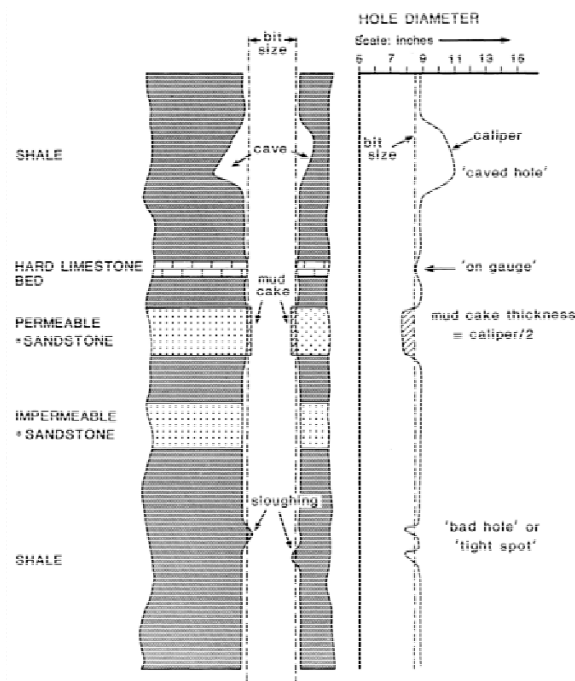


Figure A- 1: The caliper log showing some typical responses. (From Rider, 2002).

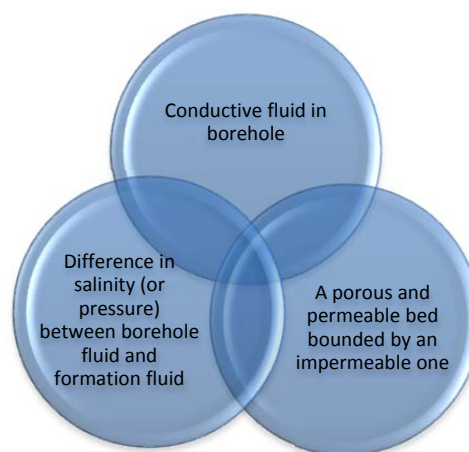


Figure A- 2: Conditions required to produce an SP response.

1 Rider, M. (2006) The Geological Interpretation of Well Logs, *Rider-French Consulting, Ltd.*, 280pp.

The SP log can be qualitatively used for permeability recognition. SP deflections from the shale base line commonly indicate the presence of a permeable bed. The magnitude and direction of the deflection is dependent upon the relative resistivity (or salinity) values of the borehole fluid and the formation fluid. If the formation fluid resistivity is less than the borehole fluid resistivity, then the relative SP values will decrease in a porous, coarse-grained unit. Alternately, if the formation fluid resistivity is greater than the borehole fluid resistivity, the relative SP values will increase in the same body, and the curve shape is referred to as a "reversed SP". If both fluid resistivities are equal, no SP deflection will occur.

## GAMMA RAY LOGS

The gamma ray log is a passive instrument that measures the amount of naturally occurring radioactivity from geologic units within the borehole. Commonly occurring radioelements include potassium, thorium, and uranium; the two former elements are predominant within a common fine-grained rock sequence. The gamma ray log is also an excellent lithologic indicator because fine-grained clays and shales contain a higher radioelement concentration than limestones or sands. Gamma ray values are often used to assess the percentage of clay materials (indurated or non-indurated) that are present within a formation by utilizing empirically derived equations and sand-shale base line information.

## NORMAL RESISTIVITY LOGS

Resistivity is a measure of how well an electric current passes through a material. Formation resistivity is an intrinsic property of rocks and depends on the porosity and resistivity of the interstitial fluid and rock matrix.

In sedimentary rocks, the resistivity values of shales (5 - 30 ohm-m) is generally lower than the resistivity of sandstone (30 - 100 ohm-m), which is lower than the resistivity limestone (75 - 300 ohm-m). The resistivity log often shows a picture of the overall depositional sequence in sedimentary environment. Resistivity of igneous and metamorphic rocks is extremely high when compared to resistivity in sedimentary rocks, with values that are commonly thousands of ohm-meters. Example resistivity log responses are shown in Figure A- 4.

## FLUID RESISTIVITY LOGS

of fluid resistivity, which is the reciprocal of fluid conductivity, provides data related to the concentration of dissolved solids in the fluid column. Although the quality of the fluid column may not reflect the quality of adjacent interstitial fluids, information can be quite useful when combined with other logs. For example, change in fluid resistivity associated with a water-producing zone that is corroborated by other logs may indicate the inflow of ground water.

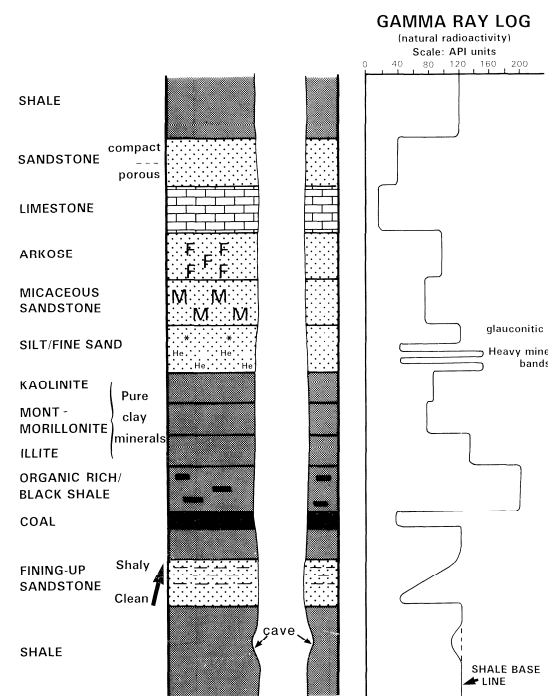


Figure A- 3: Characteristic gamma ray responses. (From Rider, 2002).

## SINGLE-POINT RESISTANCE LOGS

Single point resistance measurements are made by passing a constant current between two electrodes and recording the voltage fluctuations as the probe is moved up the borehole. The resistance variations measured in the borehole is primarily due to variations in the immediate vicinity of the downhole electrode.

The resistance log is strongly affected by the resistance of the drilling fluid and variations in borehole diameter. It is extremely useful for detecting fractures in boreholes with relatively constant diameter. In sedimentary environments, the resistance log generally follows the variations in resistivity of the formation. Shales in clay generally exhibit low values, sandstones have intermediate values, while coal and limestone beds have high resistance values.

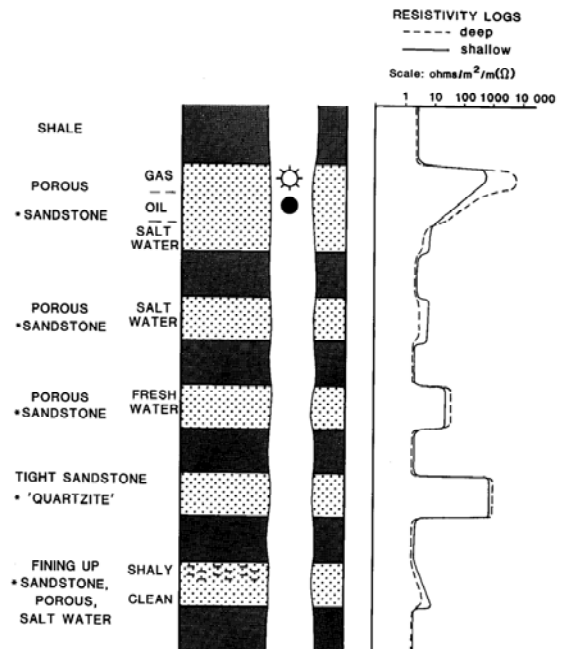


Figure A- 4: Characteristic resistivity responses. (From Rider, 2002)

## TEMPERATURE LOGS

Temperature logs measure the change in fluid temperature within the borehole as a function of depth. This log can indicate the location of water- producing strata or fracture zones within the well. The inherent assumption of this technique is that the fluids entering the borehole from water producing zones are either cooler or warmer than the fluid in the borehole. In this case, it is possible to relate a temperature anomaly to a depth range in which waters of different temperature are emanating from a water-producing/receiving or fractured lithologic unit.

## HEAT PULSE FLOWMETER (HPFM) LOGS

The heat pulse flowmeter measures the vertical flow rates within a borehole. The log may be used to identify contributing fracture zones under natural and pumping conditions. The system operates by heating a wire grid that is located between two thermistors. The heated body of water moves toward one of the thermistors under the effect of the vertical component of flow within the well. Positive and negative values on the log represent upward and downward flow, respectively. Measurements are recorded while the tool is stationary and the logs are presented as a bar graph (mud log) as shown in Figure A- 5.

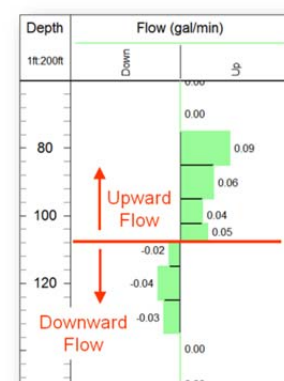


Figure A- 5: Example heat pulse flowmeter log.

A number of techniques have been attempted for measuring horizontal flow in wells without much success. The techniques may not represent the true hydrogeologic conditions due to variations in flow caused by the well.

## OPTICAL TELEVIEWER (OTV) LOGS

The optical televiewer probe combines the axial view of a downward looking digital imaging system with a precision ground hyperbolic mirror to obtain an undistorted 360° view of the borehole wall. The probe records one 360° line of pixels at 0.003-ft depth intervals. The sample circle can be divided into 720 or 360 radial samples to give 0.5° or 1° radial resolution. For this investigation, the highest radial resolution (0.5°) was used. The line of pixels is aligned with respect to True North and digitally stacked to construct a complete, undistorted, and oriented image of the borehole walls. The data are 24-bit true color and may be used for lithologic determination as part of the interpretation. Since the acquired image is digitized and properly oriented with respect to borehole deviation and tool rotation, it allows data processing to provide accurate strike and dip information of structural features. The borehole image is often shown as an “unwrapped” 360° image in which the cylindrical borehole image is sliced down the northern axis and flattened out as shown in Figure A-6.

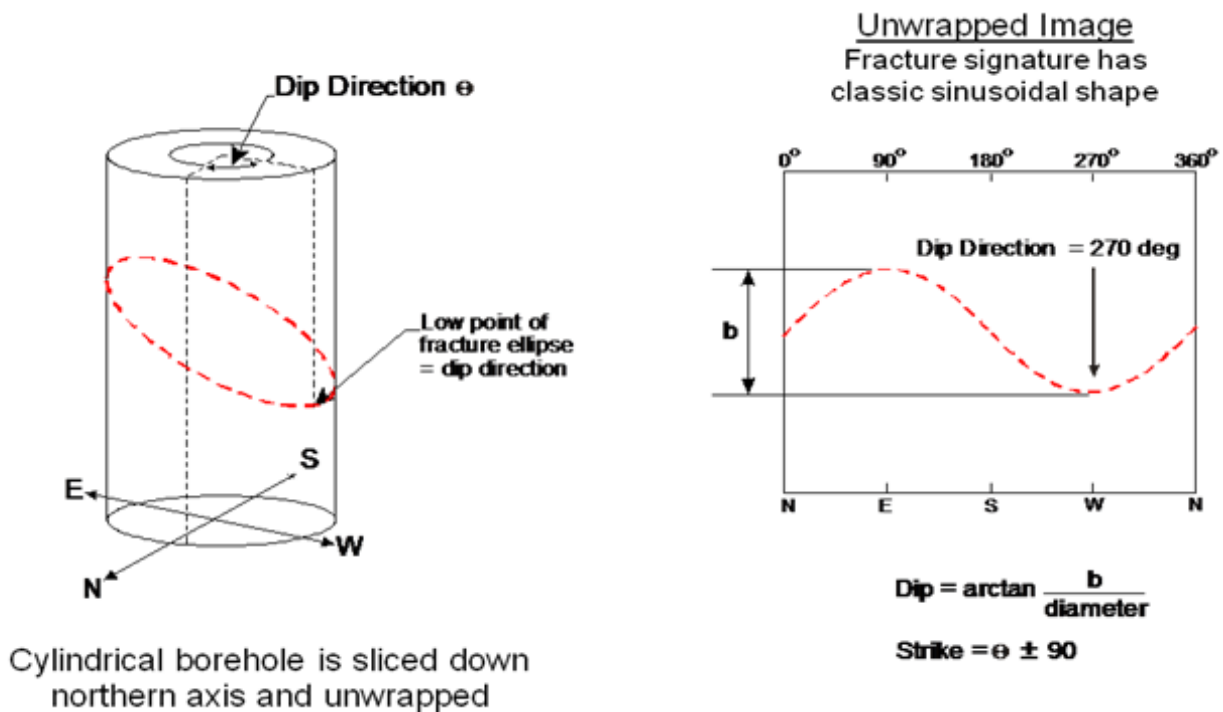


Figure A- 6: Schematic showing the sinusoidal fracture signature in the unwrapped borehole view.

## ACOUSTIC TELEVIEWER (ATV) LOGS

Acoustic televiewer provides a 360° acoustic image of the borehole walls that can be used to identify and determine the orientation of planar features such as bedding and fractures. The data can also indicate the relative degree of hardness of formation materials. As shown in Figure A-7, Ultrasonic pulses are transmitted

from a rotating transducer inside the tool. The transmitted pulses reflect off the borehole wall and return to the tool where the travel time and amplitude of the acoustic signal are measured. In order for the acoustic waves to travel to and from the borehole wall, the well must be fluid filled. Greater travel time can indicate openings in the rock. Strong amplitude suggests smooth, competent rock. Weaker amplitudes suggest rough or less competent rock.

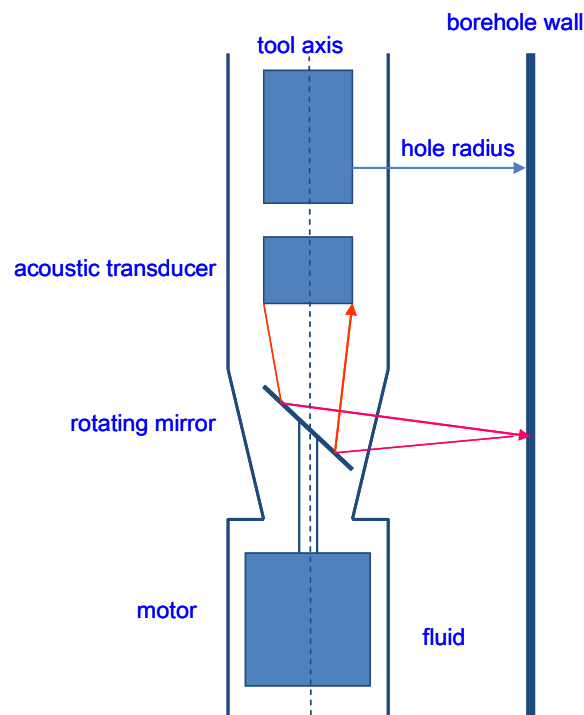
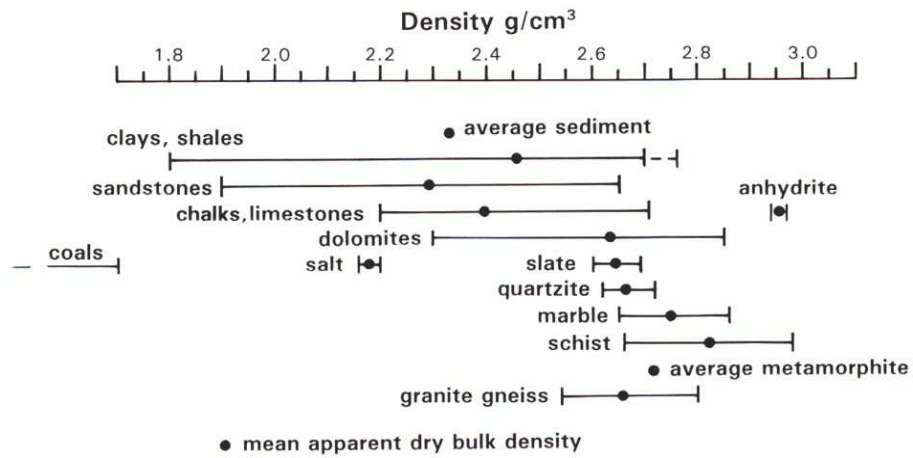


Figure A- 7: Schematic of the acoustic televiewer tool.

### DENSITY LOGS

Density logs are most often used to determine formation porosity. The probe uses a radioactive source capsule (typically containing cesium) to bombard the formation with low energy gamma rays. These rays can be thought of as particles that collide with the electrons in the formation. As these particles collide, the gamma rays are attenuated or lose energy. This loss of energy, called Compton Scattering, is directly related to the number of electrons in the formation. Therefore, the tool responds to electron density which is linearly related to bulk density. Bulk density in turn, is related to the density of the rock matrix material, the porosity of the formation, and the density of the fluids filling the pores. The density ranges for common rock types is shown below:



The density of the matrix materials and pore fluids must be known or estimated to calculate formation porosity. The porosity of the formation can be determined by:

$$\phi_{\text{density}} = \frac{\rho_{ma} - \rho_b}{\rho_{ma} - \rho_f}$$

Where:  $\rho_{ma}$  = matrix density  
 $\rho_b$  = bulk density  
 $\rho_f$  = fluid density

Densities for common matrix lithologies and fluid type are shown below:

Material	Density
Sandstone	2.65 g/cm <sup>3</sup>
Limestone	2.71 g/cm <sup>3</sup>
Dolomite	2.87 g/cm <sup>3</sup>
Fresh water	1.00 g/cm <sup>3</sup>
Salt water (200g/l)	1.13 g/cm <sup>3</sup>
Fresh water + 30% oil	0.73 - 0.78 g/cm <sup>3</sup>

## NEUTRON LOGS

Neutron logs are typically used to identify porous formations and determine their porosity. Neutron tools use a sealed radioactive source such as americium-beryllium to measure the amount of hydrogen in a formation. Fast neutrons are emitted from the tool and bombard the formation, causing collisions with the nuclei of formation materials. These collisions attenuate the neutron energy. The greatest amount of energy is lost when particles of nearly equal mass collide. Neutrons have a mass almost identical to hydrogen. Thus the attenuation of neutron energy is largely controlled by the amount of hydrogen in the formation.

Since water and oil contain a lot of hydrogen, the tool response reflects the liquid-filled porosity in clay-free formations such as sandstone and limestone. However, shales contain bound water in its crystal structure that will produce higher apparent porosity than the actual effective porosity of the formation. For this reason it is important to interpret the results in conjunction with the gamma ray log, which is good indicator of clay/shale volume.

## SONIC LOGS

Sonic logs are typically used to help identify lithology, porosity, and mechanical rock properties. The sonic tool contains acoustic transmitters and receivers. A sound pulse is generated by a transmitter and travels through the formation. One or more receivers record the sound pulse as it passes. The sonic log is simply a record of the time interval at which sound travels through 1 ft of formation. This measurement is called the interval transit time, slowness, or delta t ( $\Delta t$ ) and is the reciprocal of the velocity of the sound wave.

As the sound wave emitted by the transmitter encounters the borehole wall, 1) compressional and shear waves are generated in the formation, 2) surface wave along the borehole wall, and 3) tube waves in the borehole fluid. The first and second sound wave arrivals at the receiver are the compressional (P-wave) and shear (S-wave) arrivals, respectively. These are the most common signals used in sonic logging and their transit times vary with lithology and porosity. In addition, the interrelationship between the S- and P-waves and density can be used to calculate mechanical rock properties such as Poisson's ratio, bulk modulus, Young's modulus, and shear modulus.

Sonic-derived porosity is given by:

$$\phi_{sonic} = \frac{\Delta t_{log} - \Delta t_{ma}}{\Delta t_f - \Delta t_{ma}}$$

Where:

- $\phi_{sonic}$  = sonic derived porosity
- $\Delta t_{ma}$  = interval transit time (compressional) for matrix
- $\Delta t_f$  = interval transit time for borehole fluid



The interval transit times for common materials are shown below:

Material	$\Delta t_{ma}$ msec/ft
Sandstone	55.5
Limestone	47.6
Dolomite	43.5
Water + 20% NaCl	189
Water + 10% NaCl	208
Water (pure)	218

ATTACHMENT B  
WELL LOGS



Optical Televiwer  
Acoustic Televiwer

COMPANY: PSU		API NO.: N/A	
WELL ID: DC9			
FIELD/SITE: Shale Hills			
COUNTY: Huntingdon		STATE: PA	
LOCATION		OTHER SERVICES	
LAT:			
LONG:			
SEC:	TWP:	QUAD:	

PERMANENT DATUM: Ground Level	ELEVATION:	K.B.
LOG MEASURED FROM: Ground Level	ABOVE PERM. DATUM:	D.F.
DRILLING MEAS. FROM:	STICK UP: 1.3	G.L.

LOGGING DATE	2/8/12	2/8/12			
RUN No	1	ATV			
TYPE LOG	OTV	3			
DEPTH-DRILLER (ft)	101	101			
ARM DEPTH (ft)	100	100			
BTM LOGGED INTERVAL (ft)	89	100			
TOP LOGGED INTERVAL (ft)	5	75			
CASING SIZE/DEPTH (ft)					
CASING ARM (ft)	18.6				
BIT SIZE (inch)					
FLUID LEVEL IN HOLE (ft)	60	60			
MAG. DECLINATION (deg)	10.67 deg W	10.67 deg W			
RECORDED BY	R. Gecelesky	R. Gecelesky			
WITNESSED BY					

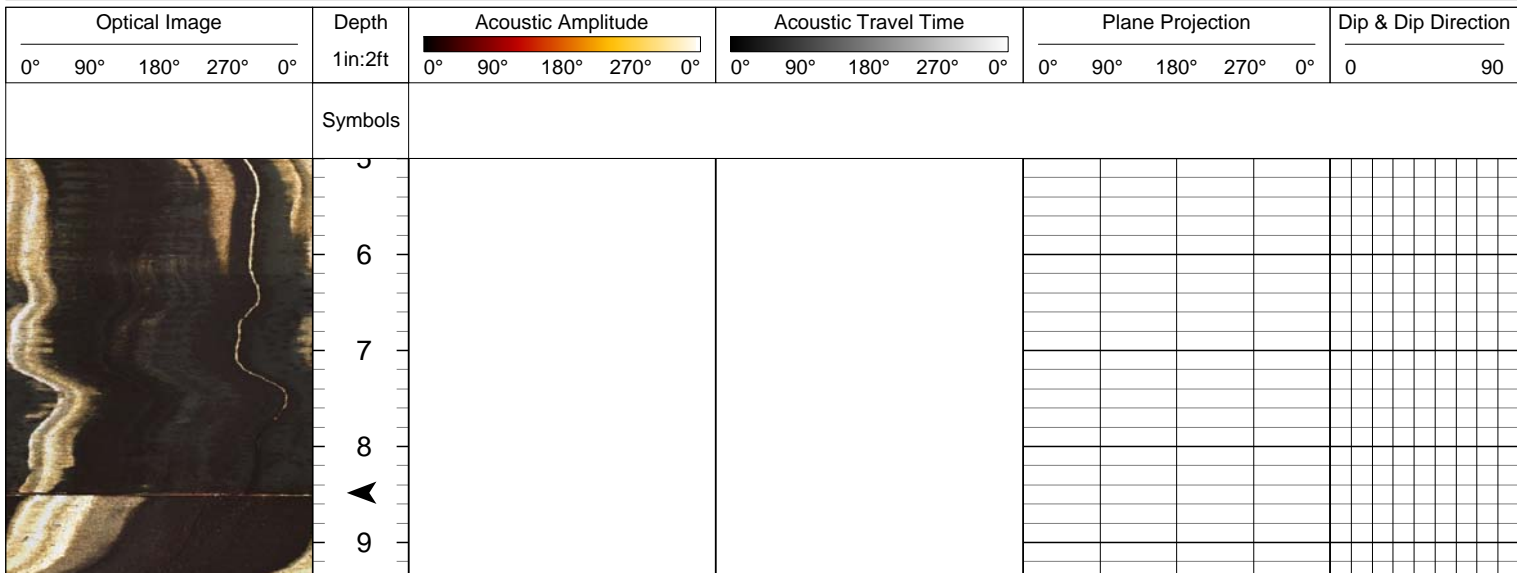
REMARKS:

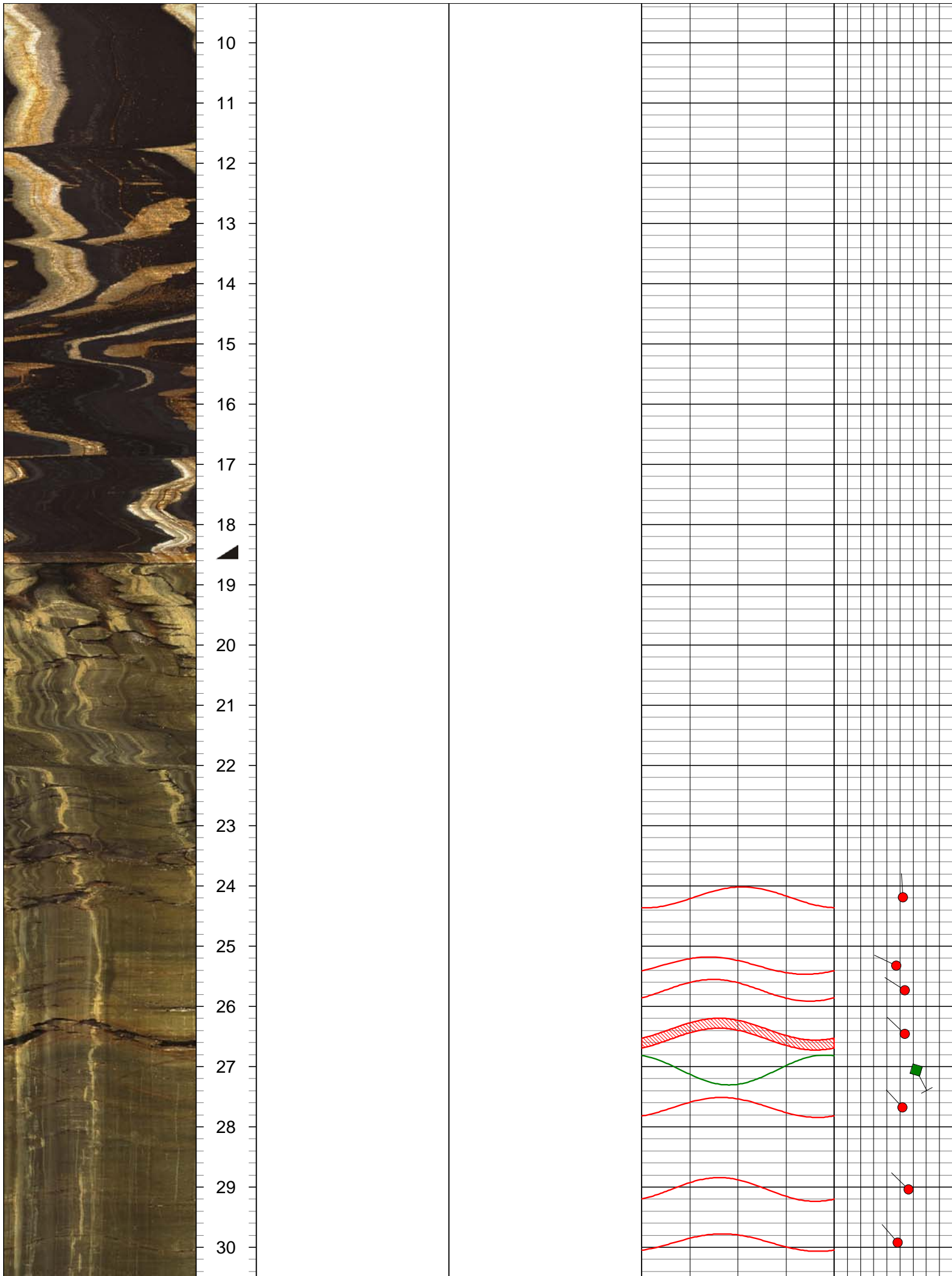
Symbols

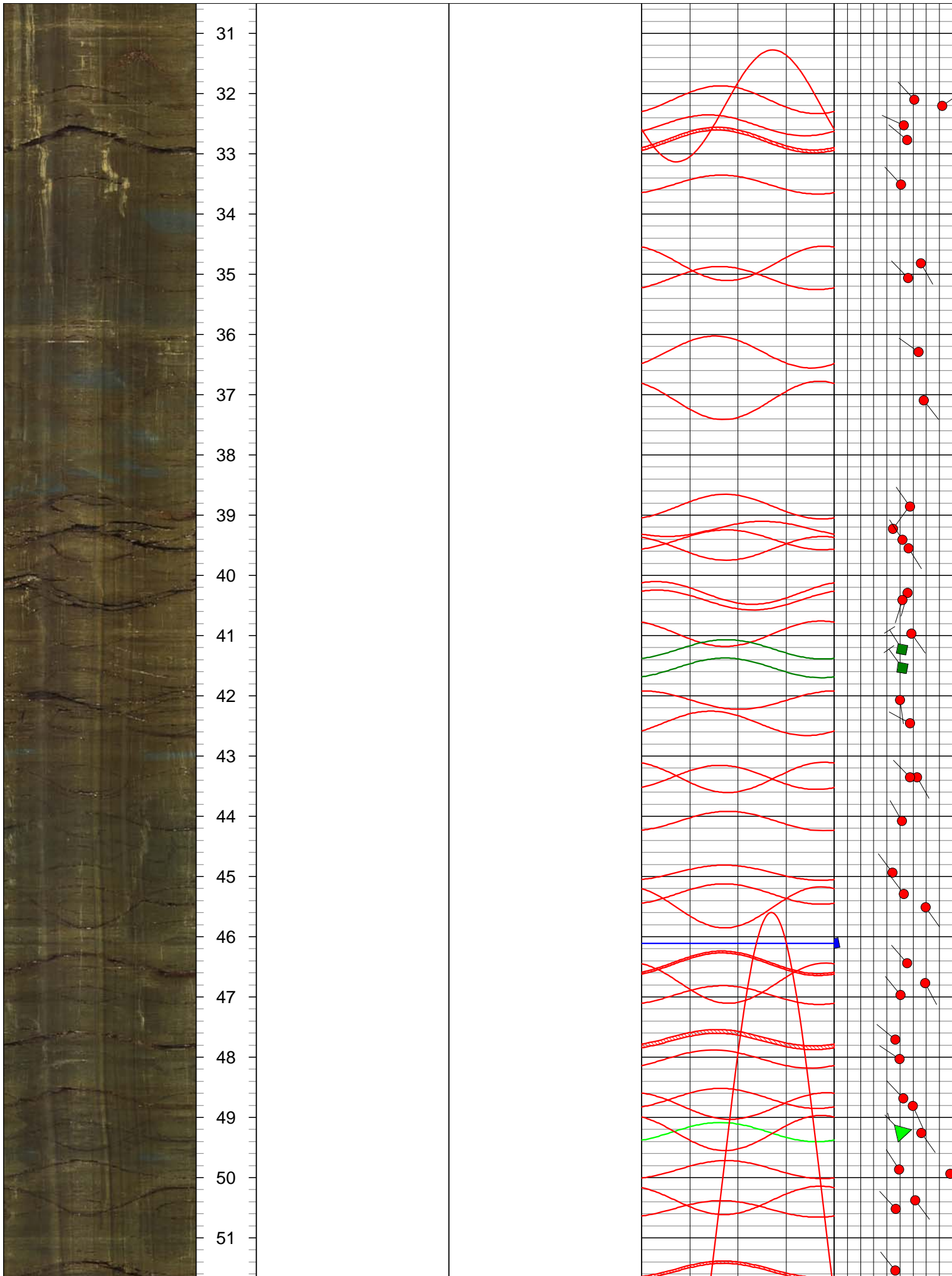
- Base of casing
- Fluid level
- Casing Joint

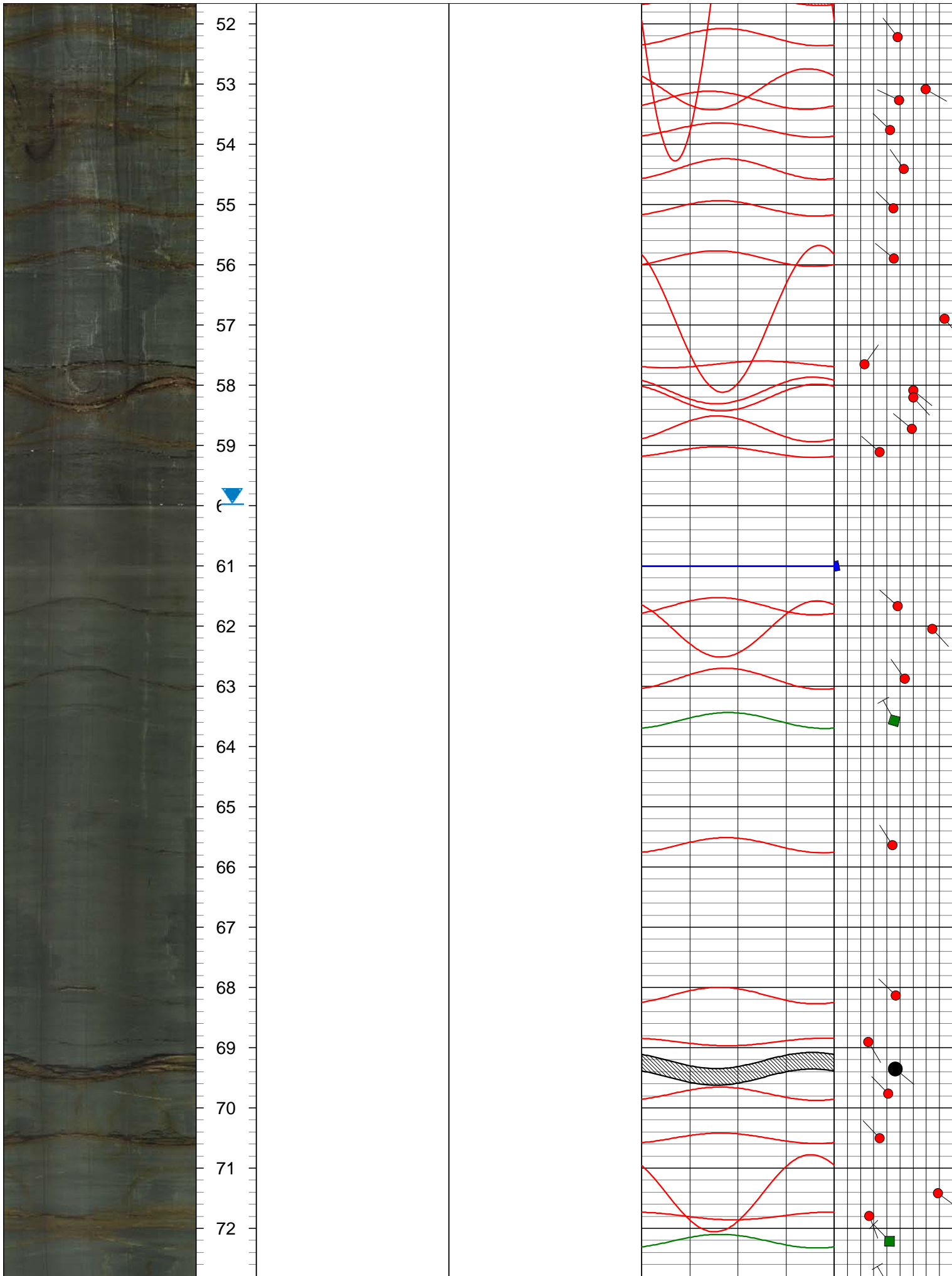
Structure

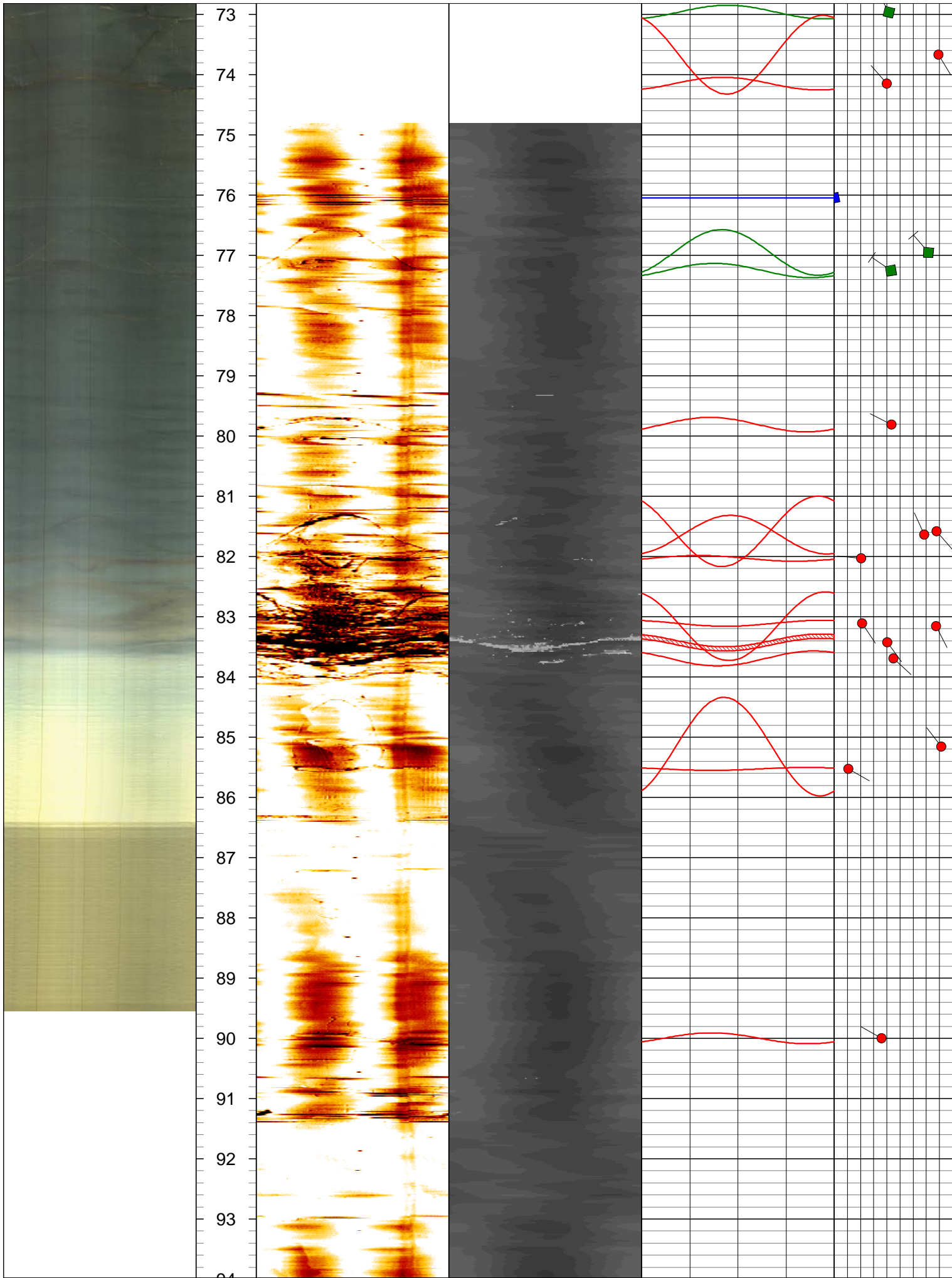
- Open Fracture
- Bedding
- Filled Fracture
- Offset Observed
- Broken/Void/Soft Zone



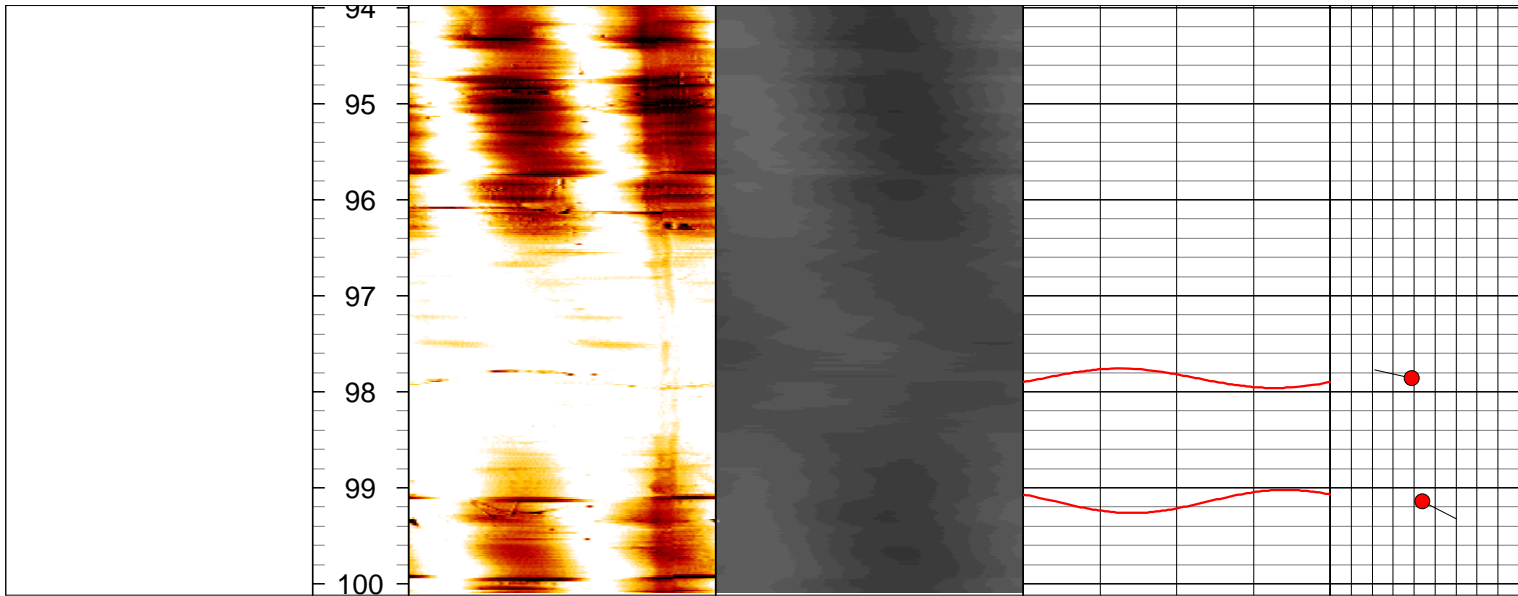














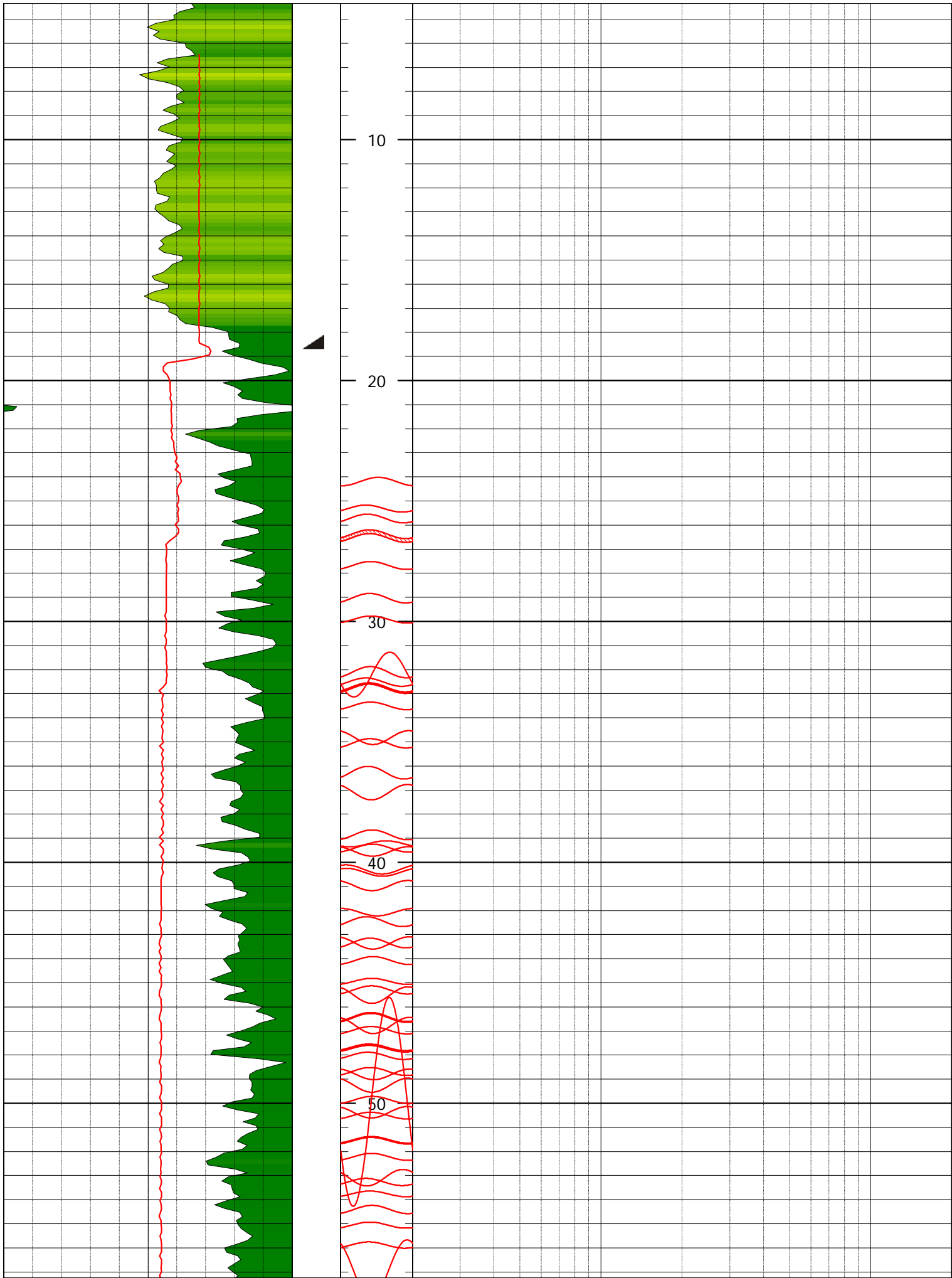


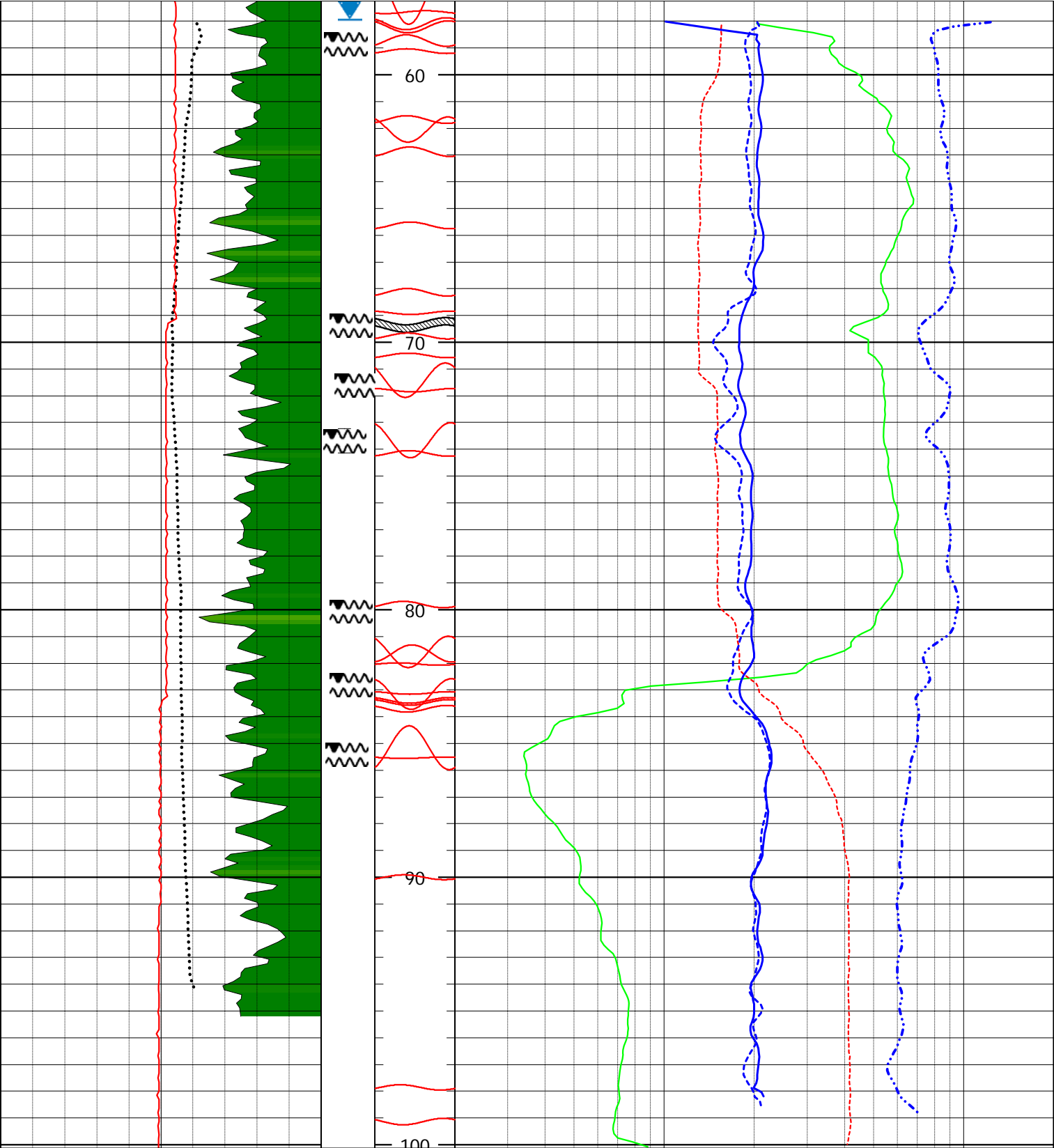
COMPANY: PSU				API NO.: N/A	
WELL ID: DC9					
FIELD/SITE: Shale Hills					
COUNTY: Huntingdon				STATE: PA	
LOCATION		OTHER SERVICES			
LAT:					
LONG:					
SEC:	TWP:	QUAD:			
PERMANENT DATUM: Ground Level		ELEVATION: ABOVE PERM. DATUM:		K.B.	
LOG MEASURED FROM: Ground Level				D.F.	
DRILLING MEAS. FROM:		STICK UP: 1.3		G.L.	
LOGGING DATE	2/8/13	2/8/13			
RUN No	2	4			
TYPE LOG	Poly	Caliper			
DEPTH-DRILLER (ft)	101	101			
ARM DEPTH (ft)	100	100			
BTM LOGGED INTERVAL (ft)	100	100			
TOP LOGGED INTERVAL (ft)	5	7			
CASING SIZE/DEPTH (ft)					
CASING ARM (ft)	18.6	18.6			
BIT SIZE (inch)					
FLUID LEVEL IN HOLE (ft)	58	58			
MAG. DECLINATION (deg)					
RECORDED BY	R. Gecelosky	R. Gecelosky			
WITNESSED BY					
REMARKS:					

### Casing shoe



<div>Gamma Ray</div> <div><div></div></div> <div>0 API 200</div>			Symbols	Depth	Fluid Resistivity		
<div>Spontaneous Potential</div> <div><div></div></div> <div>0 mV 800</div>				1in:5ft	50	Ohm-m	150
<div>Caliper</div> <div><div></div></div> <div>2 Inch 4</div>				Televue Fractures	Temperature		
			5		DegC	15	
			Single Point Resistance				
			20		Ohm	2000	
			8" Normal Resistivity				
			20		Ohm-m	2000	
			16" Normal Resistivity				
			20	Ohm-m	2000		
<div></div>				0	<div></div>		

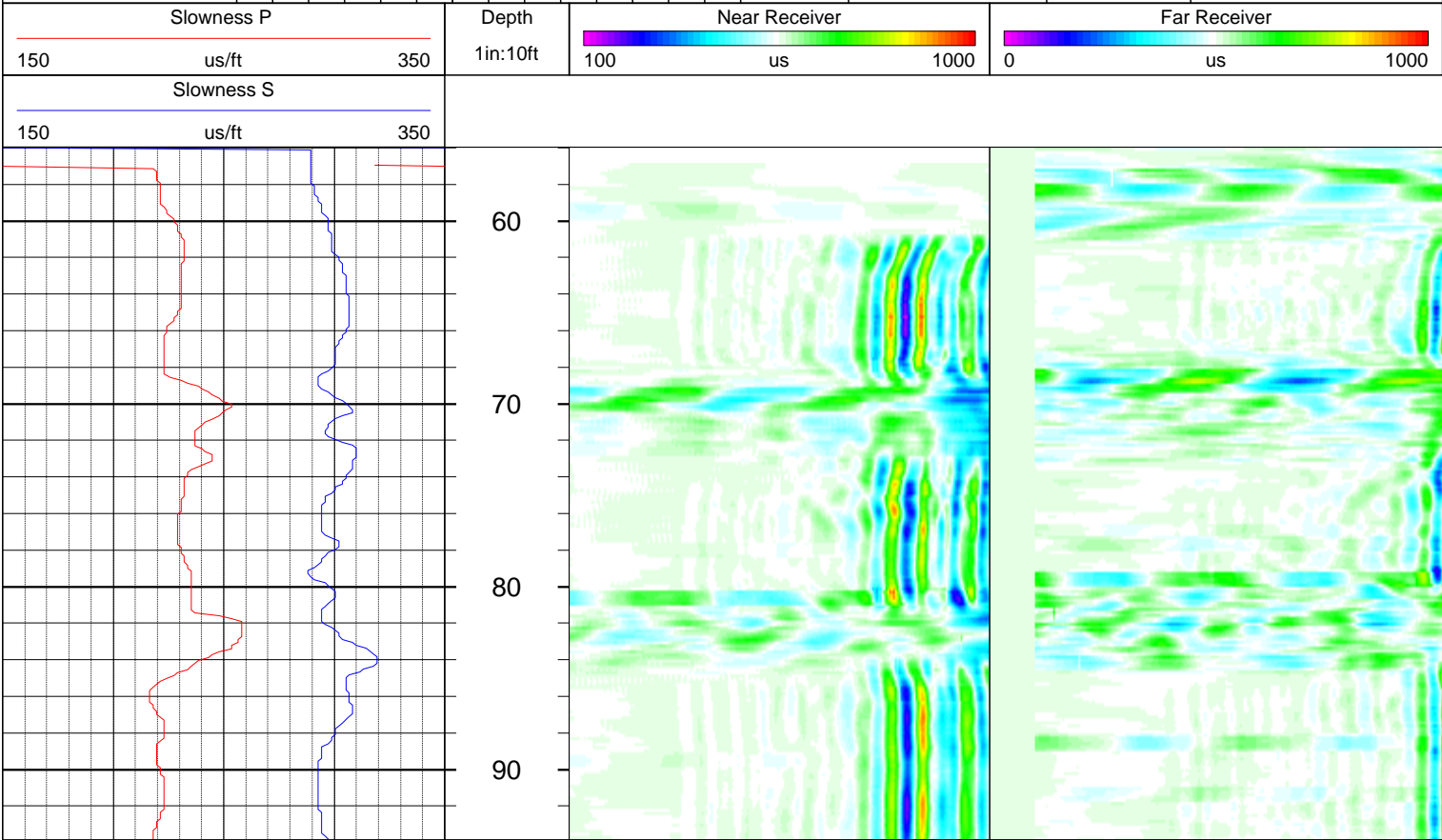






Full Waveform Sonic

COMPANY: PSU		WELL ID: DC9		API NO.: N/A	
FIELD/SITE: Shale Hills		COUNTY: Huntingdon		STATE: PA	
LOCATION		LAT:		OTHER SERVICES	
LONG:		SEC:			
TWP:		QUAD:			
PERMANENT DATUM: Ground Level		ELEVATION:		K.B.	
LOG MEASURED FROM: Ground Level		ABOVE PERM. DATUM:		D.F.	
DRILLING MEAS. FROM:		STICK UP: 1.3		G.L.	
LOGGING DATE	2/8/13				
RUN No	7				
TYPE LOG	Sonic				
DEPTH-DRILLER (ft)	101				
ARM DEPTH (ft)	100				
BTM LOGGED INTERVAL (ft)	98				
TOP LOGGED INTERVAL (ft)	58				
CASING SIZE/DEPTH (ft)					
CASING ARM (ft)	18.6				
BIT SIZE (inch)					
FLUID LEVEL IN HOLE (ft)	58				
MAG. DECLINATION (deg)					
RECORDED BY	R. Gecelesky				
WITNESSED BY					
REMARKS:					







Density Neutron Log

COMPANY: PSU		API NO.: N/A	
WELL ID: DC9			
FIELD/SITE: Shale Hills			
COUNTY: Huntingdon		STATE: PA	
LOCATION		OTHER SERVICES	
LAT:			
LONG:			
SEC:	TWP:	QUAD:	

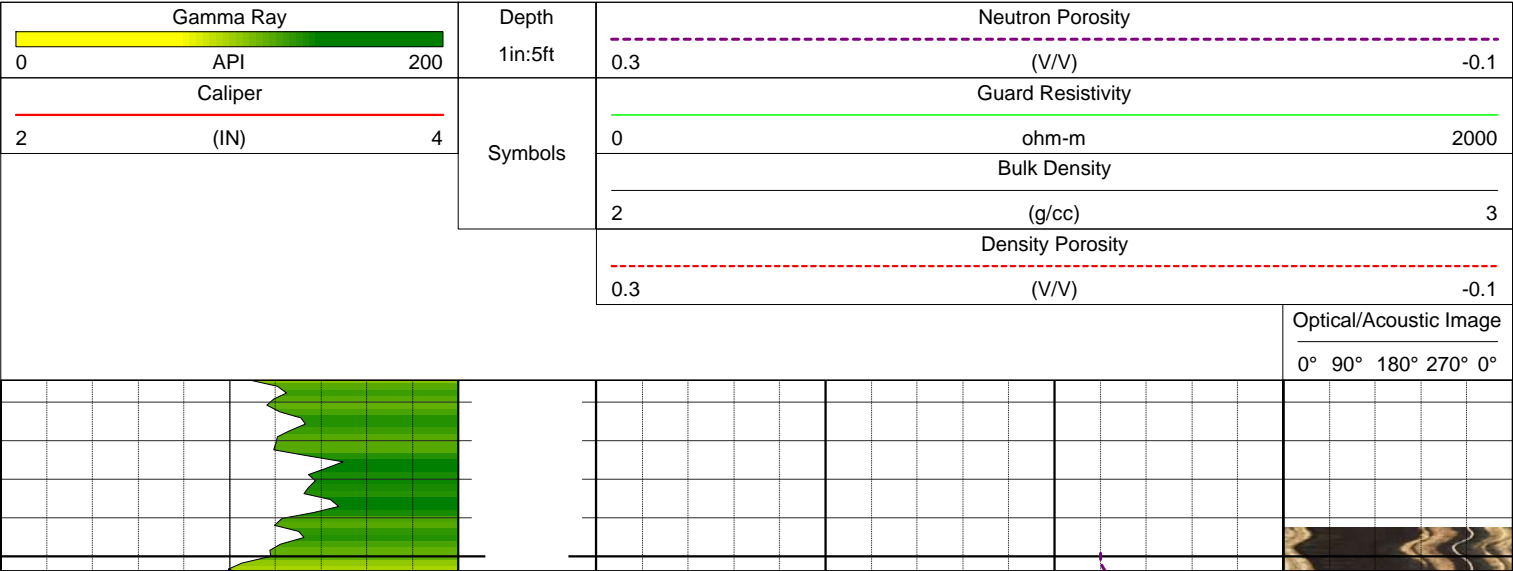
PERMANENT DATUM:	Ground Level	ELEVATION:	K.B.
LOG MEASURED FROM:	Ground Level	ABOVE PERM. DATUM:	D.F.
DRILLING MEAS. FROM:		STICK UP: 1.3	G.L.

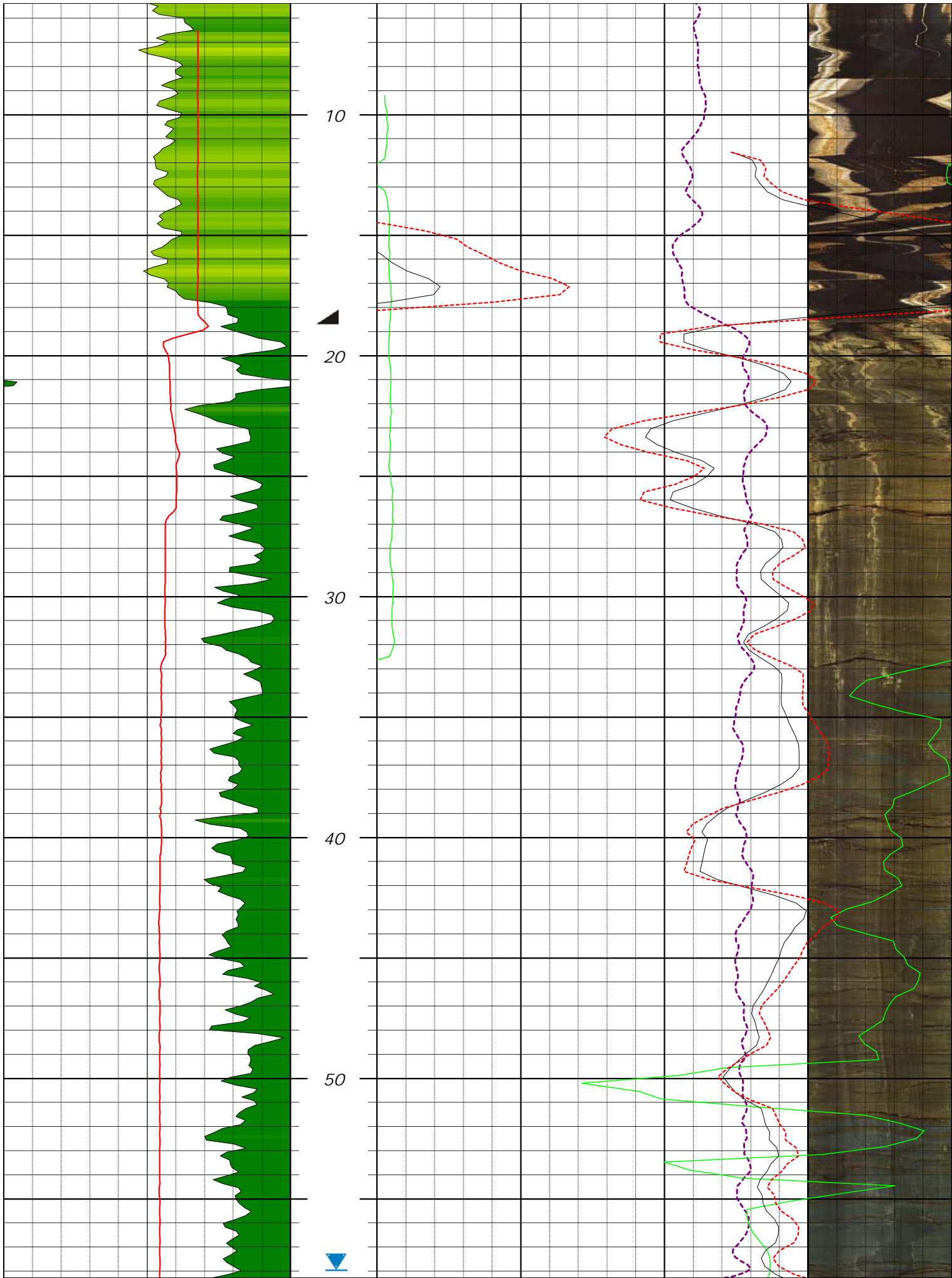
LOGGING DATE	2/8/13	2/8/13			
RUN No	5	6			
TYPE LOG	Density	Neutron			
DEPTH-DRILLER (ft)	101	101			
ARM DEPTH (ft)	100	100			
BTMLOGGED INTERVAL (ft)	100	100			
TOP LOGGED INTERVAL (ft)	10	10			
CASING SIZE/DEPTH (ft)					
CASING ARM (ft)	18.6	18.6			
BIT SIZE (inch)					
FLUID LEVEL IN HOLE (ft)	60	60			
MAG. DECLINATION (deg)					
RECORDED BY	R. Gecelesky	R. Gecelesky			
WITNESSED BY					
REMARKS:					

Symbols

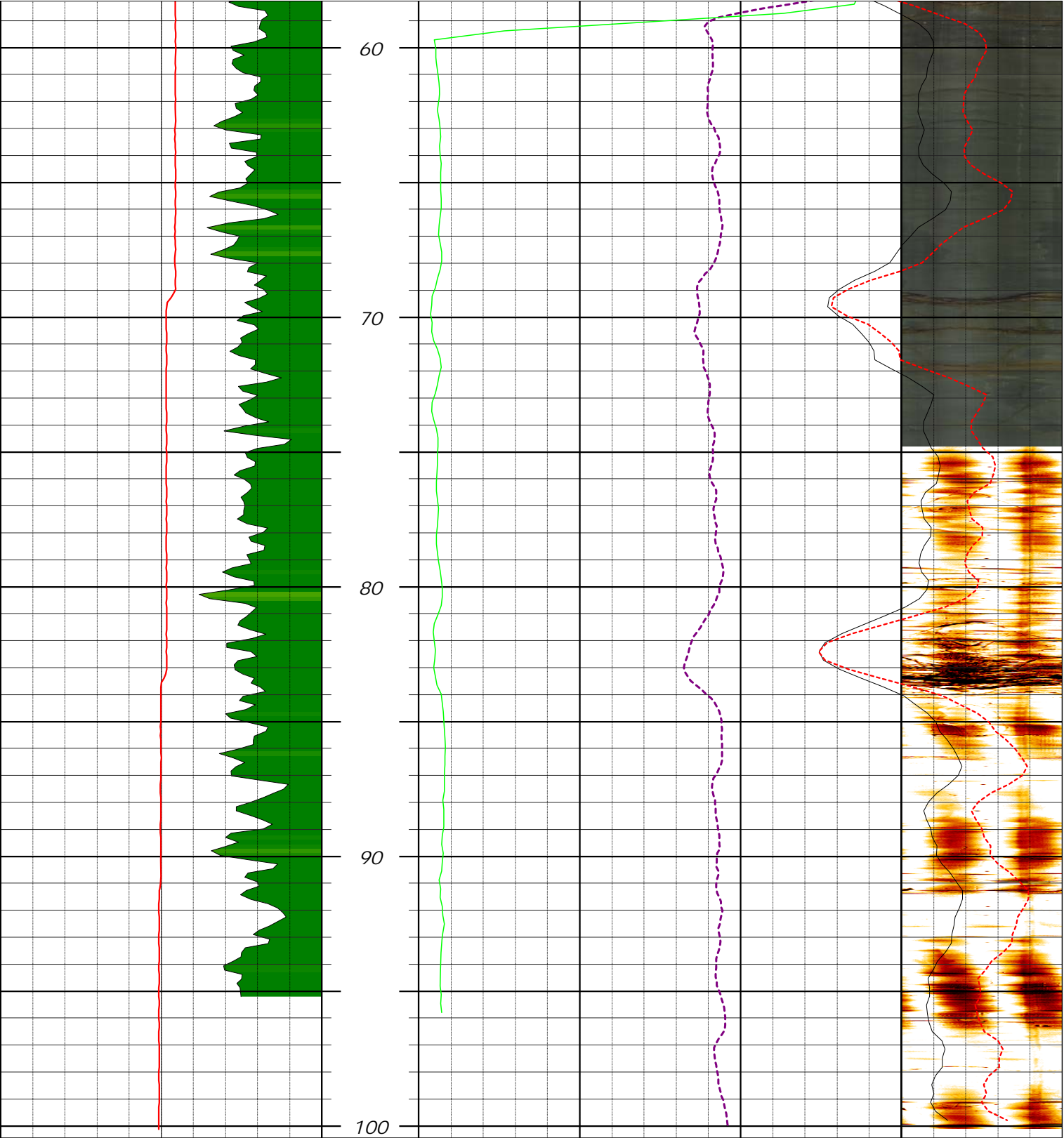
Fluid level

Casing shoe











ATTACHMENT C  
TABULATED LISTING OF PLANAR ORIENTATIONS

Planar Orientations  
DC9, Shale Hills

Well ID	Depth (feet)	Dip Dir. (deg)	Dip (deg)	Aperture (mm)	Type	Strike/Dip (Quadrant)	Strike Azimuth (Right-hand-rule)
DC9	24.19	356.74	52.14	0	Open Fracture		266.7
DC9	25.32	295.58	47.04	0	Open Fracture	N26E/47NW	205.6
DC9	25.73	303	53.58	0	Open Fracture	N33E/54NW	213.0
DC9	26.46	313.65	53.73	33.83	Open Fracture	N44E/54NW	223.7
DC9	27.06	152.42	62.27	0	Filled Fracture	N62E/62SE	62.4
DC9	27.68	318.29	51.74	0	Open Fracture	N48E/52NW	228.3
DC9	29.04	314.12	56.5	0	Open Fracture	N44E/57NW	224.1
DC9	29.92	320.14	48.18	0	Open Fracture	N50E/48NW	230.1
DC9	32.1	317.36	60.73	0	Open Fracture	N47E/61NW	227.4
DC9	32.2	54.66	82	0	Open Fracture	N35W/82NE	324.7
DC9	32.53	294.66	53.05	0	Open Fracture	N25E/53NW	204.7
DC9	32.77	310.41	55.6	9.44	Open Fracture	N40E/56NW	220.4
DC9	33.51	318.29	50.6	0	Open Fracture	N48E/51NW	228.3
DC9	34.82	149.64	65.82	0	Open Fracture	N60E/66SE	59.6
DC9	35.07	315.97	56.15	0	Open Fracture	N46E/56NW	226.0
DC9	36.29	305.78	64.14	0	Open Fracture	N36E/64NW	215.8
DC9	37.1	141.76	67.93	0	Open Fracture	N52E/68SE	51.8
DC9	38.86	325.7	57.71	0	Open Fracture	N56E/58NW	235.7
DC9	39.23	36.13	44.48	0	Open Fracture	N54W/44NE	306.1
DC9	39.41	327.55	51.96	0	Open Fracture	N58E/52NW	237.6
DC9	39.55	147.32	56.68	0	Open Fracture	N57E/57SE	57.3
DC9	40.29	195.97	55.68	0	Open Fracture	N74W/56SW	106.0
DC9	40.41	197.36	51.96	0	Open Fracture	N73W/52SW	107.4
DC9	40.97	145.01	58.55	0	Open Fracture	N55E/59SE	55.0
DC9	41.23	327.55	51.43	0	Filled Fracture	N58E/51NW	237.6
DC9	41.53	324.77	51.75	0	Filled Fracture	N55E/52NW	234.8
DC9	42.07	171.41	50.01	0	Open Fracture	N81E/50SE	81.4
DC9	42.45	298.36	57.57	0	Open Fracture	N28E/58NW	208.4
DC9	43.35	150.1	63.03	0	Open Fracture	N60E/63SE	60.1
DC9	43.36	315.97	57.44	0	Open Fracture	N46E/57NW	226.0
DC9	44.08	330.33	51.41	0	Open Fracture	N60E/51NW	240.3
DC9	44.94	323.85	44.35	0	Open Fracture	N54E/44NW	233.9
DC9	45.29	323.85	52.82	0	Open Fracture	N54E/53NW	233.9
DC9	45.51	144.54	69.48	0	Open Fracture	N55E/69SE	54.5
DC9	46.11	349.33	0	0	Bedding	N79E/0NW	259.3
DC9	46.44	319.21	55.56	6.33	Open Fracture	N49E/56NW	229.2
DC9	46.77	151.96	68.96	0	Open Fracture	N62E/69SE	62.0
DC9	46.97	321.07	50.37	0	Open Fracture	N51E/50NW	231.1
DC9	47.71	310.41	46.54	13.86	Open Fracture	N40E/47NW	220.4
DC9	48.03	303.92	49.64	0	Open Fracture	N34E/50NW	213.9
DC9	48.69	316.9	52.45	0	Open Fracture	N47E/52NW	226.9
DC9	48.81	154.74	59.7	0	Open Fracture	N65E/60SE	64.7
DC9	49.24	316.43	51.06	0	Fault	N46E/51NW	226.4
DC9	49.26	145.01	66.14	0	Open Fracture	N55E/66SE	55.0
DC9	49.87	327.55	49.26	0	Open Fracture	N58E/49NW	237.6
DC9	49.94	51.88	88.3	0	Open Fracture	N38W/88NE	321.9
DC9	50.38	142.69	61.49	0	Open Fracture	N53E/61SE	52.7
DC9	50.52	318.29	46.92	0	Open Fracture	N48E/47NW	228.3
DC9	51.54	321.99	46.58	9.24	Open Fracture	N52E/47NW	232.0
DC9	52.22	322.92	48.18	0	Open Fracture	N53E/48NW	232.9
DC9	53.08	119.52	69.44	0	Open Fracture	N30E/69SE	29.5
DC9	53.27	295.58	49.26	0	Open Fracture	N26E/49NW	205.6
DC9	53.77	315.04	42.51	0	Open Fracture	N45E/43NW	225.0

Planar Orientations  
DC9, Shale Hills

Well ID	Depth (feet)	Dip Dir. (deg)	Dip (deg)	Aperture (mm)	Type	Strike/Dip (Quadrant)	Strike Azimuth (Right-hand-rule)
DC9	54.41	324.77	53.04	0	Open Fracture	N55E/53NW	234.8
DC9	55.06	315.04	44.82	0	Open Fracture	N45E/45NW	225.0
DC9	55.9	309.48	45.24	0	Open Fracture	N39E/45NW	219.5
DC9	56.9	140.84	83.97	0	Open Fracture	N51E/84SE	50.8
DC9	57.65	35.2	23.16	0	Open Fracture	N55W/23NE	305.2
DC9	58.08	129.25	60.02	0	Open Fracture	N39E/60SE	39.3
DC9	58.2	137.59	60.02	0	Open Fracture	N48E/60SE	47.6
DC9	58.72	310.41	59.04	0	Open Fracture	N40E/59NW	220.4
DC9	59.11	311.34	34.57	0	Open Fracture	N41E/35NW	221.3
DC9	61	349.33	0	0	Bedding	N79E/ONW	259.3
DC9	61.67	312.26	48.14	0	Open Fracture	N42E/48NW	222.3
DC9	62.05	137.59	74.62	0	Open Fracture	N48E/75SE	47.6
DC9	62.87	325.7	53.74	0	Open Fracture	N56E/54NW	235.7
DC9	63.56	331.26	45.75	0	Filled Fracture	N61E/46NW	241.3
DC9	65.64	327.55	44.42	0	Open Fracture	N58E/44NW	237.6
DC9	68.13	314.12	46.92	0	Open Fracture	N44E/47NW	224.1
DC9	68.91	149.18	26.05	0	Open Fracture	N59E/26SE	59.2
DC9	69.35	128.33	46.54	64.74	Broken/Void/Soft Zone	N38E/47SE	38.3
DC9	69.76	315.97	41.11	0	Open Fracture	N46E/41NW	226.0
DC9	70.5	316.9	34.44	0	Open Fracture	N47E/34NW	226.9
DC9	71.42	125.55	78.85	0	Open Fracture	N36E/79SE	35.6
DC9	71.79	159.37	26.5	0	Open Fracture	N69E/27SE	69.4
DC9	72.21	315.97	42.11	0	Filled Fracture	N46E/42NW	226.0
DC9	72.96	329.41	41.61	0	Filled Fracture	N59E/42NW	239.4
DC9	73.67	148.71	79.02	0	Open Fracture	N59E/79SE	58.7
DC9	74.15	320.14	40.08	0	Open Fracture	N50E/40NW	230.1
DC9	76.05	349.33	0	0	Bedding	N79E/ONW	259.3
DC9	76.95	319.21	71.61	0	Filled Fracture	N49E/72NW	229.2
DC9	77.25	304.85	43.08	0	Filled Fracture	N35E/43NW	214.9
DC9	79.81	296.97	43.55	0	Open Fracture	N27E/44NW	207.0
DC9	81.58	138.98	77.8	0	Open Fracture	N49E/78SE	49.0
DC9	81.64	335.89	68.5	0	Open Fracture	N66E/69NW	245.9
DC9	82.03	275.2	20.45	0	Open Fracture	N5E/20NW	185.2
DC9	83.11	145.93	21.28	0	Open Fracture	N56E/21SE	55.9
DC9	83.16	152.42	77.48	0	Open Fracture	N62E/77SE	62.4
DC9	83.43	143.62	40.29	18.13	Open Fracture	N54E/40SE	53.6
DC9	83.69	131.57	44.87	0	Open Fracture	N42E/45SE	41.6
DC9	85.16	322.92	81.31	0	Open Fracture	N53E/81NW	232.9
DC9	85.53	119.52	10.7	0	Open Fracture	N30E/11SE	29.5
DC9	90	299.75	35.89	0	Open Fracture	N30E/36NW	209.8
DC9	97.85	283.08	38.86	0	Open Fracture	N13E/39NW	193.1
DC9	99.14	116.74	43.95	0	Open Fracture	N27E/44SE	26.7